Entanglement Generation by Fock-State Filtration

K. J. Resch,[1,2] J. L. O'Brien,[1,3] T. J. Weinhold,[1] K. Sanaka,[4] B. P. Lanyon,[1] N. K. Langford,[1] and A. G. White[1]

[1]*Department of Physics & Centre for Quantum Computer Technology, University of Queensland, Brisbane, QLD 4072, Australia*
[2]*Department of Physics & Institute for Quantum Computing, University of Waterloo, Waterloo, ON N2L 3G1, Canada*
[3]*H. H. Wills Physics Laboratory & Department of Electrical and Electronic Engineering, University of Bristol, Bristol, BS8 1UB, United Kingdom*
[4]*E. L. Ginzton Laboratory, Stanford University, Stanford, California 94305, USA*

(Received 31 July 2006; published 16 May 2007)

We demonstrate a Fock-state filter which is capable of preferentially blocking single photons over photon pairs. The large conditional nonlinearities are based on higher-order quantum interference, using linear optics, an ancilla photon, and measurement. We demonstrate that the filter acts coherently by using it to convert unentangled photon pairs to a path-entangled state. We quantify the degree of entanglement by transforming the path information to polarization information; applying quantum state tomography we measure a tangle of $T = (20 \pm 9)\%$.

DOI: 10.1103/PhysRevLett.98.203602 PACS numbers: 42.50.Dv, 03.65.Wj, 03.67.Mn, 42.50.Nn

In practice it is extremely difficult to make one photon coherently influence the state of another. The optical nonlinearities required are orders of magnitude beyond those commonly achieved with current technology. Strong effective nonlinearities can be induced in linear optical systems by combining quantum interference and projective measurement [1], opening the possibility of scalable linear-optical quantum computation. Such measurement-induced nonlinearities have had high impact in quantum information, notably in optical quantum logic gate experiments [2,3] and in exotic state production [4,5].

Most schemes achieve an effective nonlinearity via lowest-order nonclassical interference, with one photon per mode input to a beam splitter. Higher-order nonclassical interference, where more than one photon is allowed per mode, enables additional control [1]. An ancilla photon has been used to conditionally control the phase of a two-photon path-entangled state [2], and to conditionally absorb either one- or two-photon states [6]. Applied to superpositions, higher-order interference is predicted to act as a Fock-state filter [7,8], conditionally absorbing only terms with a specified number of photons. In this Letter, we prove that conditional absorption is coherent by applying it to a superposition, and experimentally generating a path-entangled state. We quantify the entanglement by transforming path information to polarization, and applying quantum state tomography [9].

The Fock-state filter uses nonclassical interference at a single, polarization-independent, beam splitter of reflectivity R. Consider the beam splitter in Fig. 1 with $n + 1$ photons incident: n in mode a, and 1 (the ancilla) in mode b. There are $n + 1$ possible ways for there to be one and only one photon in mode d: all the input photons can be reflected, with probability amplitude $\sqrt{R}^{n+1}$, or there are n ways for a photon from each input to be transmitted and the rest reflected, $n(1 - R)\sqrt{R}^{n-1}$. Assuming indistinguishable photons, the probability amplitude for detecting one and only one photon in mode d is $A(n) = R^{(n-1)/2}[R - n(1 - R)]$ [6,7,10]. Note that the probability $P(n) = |A(n)|^2$ can be zero for any single choice of n, when $R = n/(n + 1)$; for all other n, $P > 0$ [6]. Hong-Ou-Mandel interference is the lowest-order case, where $P = 0$ when $n = 1$ and $R = \frac{1}{2}$ [11]: the detector in mode d is never hit by a single photon. If a superposition of number states is input into mode a and a single photon is detected in mode d, then the output state in mode c cannot contain $|1\rangle$.

The Fock-state filter could be tested by creating a number-state superposition, applying the filter, and tomographically measuring the resulting state. In practice, each step of this naïve approach is impractical: creating nonclassical number-state superpositions is onerous [4,12] and they are easily destroyed by loss; the Fock-state filter requires an ancilla photon on demand and a perfect-

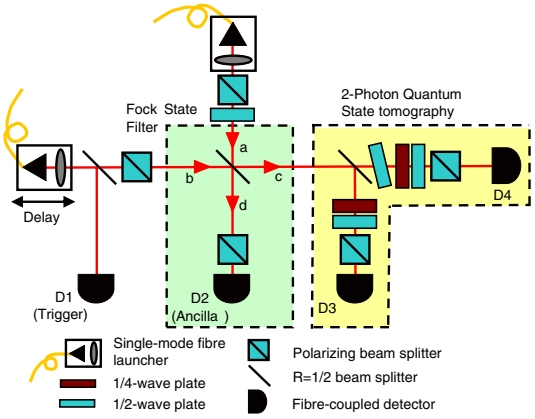

FIG. 1 (color online). The Fock-state filter: a device that blocks the passage of single photons, but allows the coherent passage of photon pairs. As described in the text, a probabilistic Fock-state filter can be created by combining a 50% beam splitter, ancilla photon, quantum interference, and measurement.

efficiency number-resolving detector; and tomography needs high-efficiency homodyne measurement.

Our experiment alleviates each difficulty. We use double-pair emission from parametric down conversion to generate a pair of polarized two-photon states in separate spatial modes. Down conversion is often problematic since it emits photon pairs probabilistically, and can emit more than one pair at a time. However, in some cases double-pair emission is beneficial [13], or essential [14]. Double-pair emission provides input two-photon states in mode a and single, ancillary, photons in mode b: we create the superposition in mode a by rotating its polarization,

$$|2_H, 0_V\rangle_a \rightarrow \cos^2\theta|2_H, 0_V\rangle_a + \sin^2\theta|0_H, 2_V\rangle_a + \sqrt{2}\cos\theta\sin\theta|1_H, 1_V\rangle_a, \quad (1)$$

where θ is the polarization angle relative to horizontal. We create a horizontally polarized ancilla photon in mode b by passing the two-photon state through a 50% beam splitter and triggering on detection events from the output mode of the beam splitter, see Fig. 1. The trigger photon is measured in coincidence with the three photons output from the beam splitter: if a photon is lost then it cannot contribute to the fourfold coincidence signal.

The Fock-state filter acts nonlinearly only on light with the same polarization as the ancilla, horizontal in this case. The amplitude given in Eq. (1) determines the transformation on horizontally polarized components of the state, $|n_H\rangle|1_H\rangle \rightarrow A(n_H)|n_H\rangle|1_H\rangle + \ldots$; in contrast, the vertically polarized components are transformed as, $|n_V\rangle|1_H\rangle \rightarrow R^{(n_V+1)/2}|n_V\rangle|1_H\rangle + \ldots$. Measurement of a single horizontally polarized photon in mode d selects only the first terms of these transformations (the latter amplitude represents the only way that a horizontally polarized photon can be detected in mode d). Noting that the conditional transformation is not unitary, and applying this to the terms in Eq. (1) we find, $|2_H, 0_V\rangle_a \rightarrow -|2_H, 0_V\rangle_c/2\sqrt{2}$, $|1_H, 1_V\rangle_a \rightarrow 0$, and $|0_H, 2_V\rangle_a \rightarrow |0_H, 2_V\rangle_c/2\sqrt{2}$, and the state of mode c conditioned on a horizontal photon detected in mode d is,

$$\frac{-\cos^2\theta|2_H, 0_V\rangle_c + \sin^2\theta|0_H, 2_V\rangle_c}{(\cos^4\theta + \sin^4\theta)^{1/2}}. \quad (2)$$

The final state can be tuned between separable and entangled number-path states simply by adjusting the input polarization θ. In the case, $\theta = \pi/4$, this is the lowest-order NOON state [15], $(|2_H, 0_V\rangle - |0_H, 2_V\rangle)/\sqrt{2}$ [16,17].

Note that the vertical polarization is a stable phase reference for the nonlinear sign change of the horizontal components, removing the need for a stable homodyne measurement. The final state is transformed from one to two spatial modes by a 50% beam splitter: mapping the path-entanglement into polarization-entanglement lets us characterize the state with quantum state tomography of the polarization, with all of its attendant advantages [9].

Our down-conversion source was a BBO (β-barium borate) nonlinear crystal cut for noncollinear type-I frequency conversion (410 nm → 820 nm), pumped by a frequency-doubled titanium sapphire laser. The down-converted light was coupled into two single-mode optical fibers, which when connected directly to FC-connectorized single-photon counting modules yielded coincidence rates of 30 kHz and singles rates of 220 kHz. Before coupling back into free-space, the polarization of the light was manipulated in-fiber using "bat-ears" to maximize transmission through horizontal polarizers. Light in mode b was split by a 50% beam splitter, where one output mode was coupled directly into a single-mode fiber coupled detector, D1, which acted as a trigger. The remaining light passed through a horizontal polarizer and is combined on a second 50% beam splitter with light from mode a, which is first passed through a horizontal polarizer and half-wave plate to rotate the polarization, as described in Eq. (1). Mode d is directly detected at D2; mode c is split into two modes by a 50% beam splitter, each mode is polarization analyzed using a quarter- and half-wave plate and polarizer. We use D3 and D4 to perform a tomographically complete

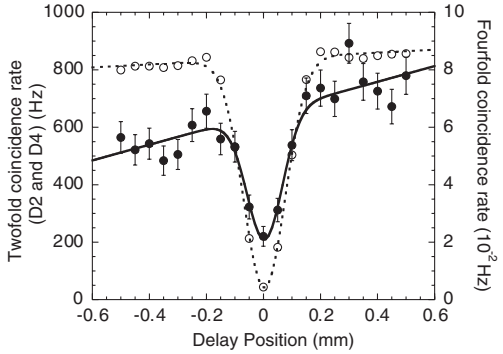

FIG. 2. Quantum interference in two- and fourfold coincidence counts as a function of the longitudinal position of the input fiber coupler for mode b. At zero delay, we see marked preferential absorption of single-photon over two-photon states in mode c, as indicated by the larger dip in two- over fourfold counts. The two- and fourfold raw visibilities are (95.20 ± 0.02)% and (68 ± 5)%, respectively; correcting for background as described in the text, the twofold visibility becomes (99.6 ± 0.1)% (error bars are smaller than the points in the twofold case and are not shown). The visibilities are in excellent agreement with the theoretically expected two- and four-visibilities of 100% and 66.7% [6,11,18]. The input coupler was scanned 1 mm in 630 s: to mitigate drift effects the scan was repeated 63 times, leading to an integration time of 31.5 min per point. The slopes in the data are due to longitudinal-position-dependent coupling to the detectors; the trigger detector was particularly sensitive in this respect, leading to a large slope in the fourfolds; the twofolds show a much smaller slope as the trigger detector plays no role in that data. The visibilities were obtained from curve fits to products of a Gaussian and a linear function.

set of two-qubit measurements, $\{H, V, D, R\} \otimes \{H, V, D, R\}$, in coincidence with the trigger and ancilla detectors, D1 and D2. The resulting density matrices are reconstructed using the maximum-likelihood technique [9]. All optical paths between fiber couplers to detectors were made approximately equal (~50 cm) to facilitate high-efficiency single-mode to single-mode fiber coupling. The tilted half-wave plate in the D4 arm, set with its optic axis horizontal, compensated beam splitter birefringence.

Nonclassical interference is the heart of the Fock-state filter. We characterized this by setting the polarization of mode a to horizontal, matching that of mode b, and setting analyzers at D3, D4 to horizontal. Figure 2 shows experimentally measured twofold coincidence counts, in this case between detectors D2 and D4 (open circles), and the fourfold coincidence counts, between D1, D2, D3, and D4 (solid circles), as a function of the longitudinal position of the input fiber coupler for mode b.

As D2 and D4 detect the two outputs of the beam splitter, the twofolds show the standard Hong-Ou-Mandel interference dip [11], with a raw visibility of $V_1 = (95.20 \pm 0.02)\%$. To estimate the performance of the Fock-state filter we must consider the events from double-pair emission. We can estimate these by blocking mode a and b in turn and measuring the twofold coincidences between detectors D2 and D4, 5.8 ± 0.16 Hz and 30.9 ± 0.5 Hz, respectively. Summing these gives an estimate of the number of twofold coincidences due to the two-photon terms in modes a and b, (36.7 ± 0.5) Hz. These coincidences act as a background; subtracting them gives a corrected visibility of $V_1' = (99.6 \pm 0.1)\%$.

The fourfold coincidence counts in Fig. 2 display a higher-order nonclassical interference effect with visibility $V_2 = (68 \pm 5)\%$, which agrees with the expected value of 66.7% [6]. Note that the interference visibility is much larger for the $n = 1$ input state, as measured by the twofold coincidences, than the $n = 2$ input state, as measured by the fourfold coincidences. At the center of the interference dip, single photons are removed from an input state with much higher probability than pairs of photons: this is the action of the Fock-state filter.

The visibilities, V_1' and V_2, set an upper bound to the performance of the Fock-state filter. Ideally, the probability of transmission when the ancilla and n-photon inputs are distinguishable is $Q(n) = R^{n+1} + nR^{n-1}(1 - R)^2$ [6]. The nonlinear absorption probability $P(n)$ is modified by the visibilities as $P'(n) = (1 - V_n)Q(n)$. We estimate the filter's efficiency of blocking single photons, $P'(2)/P'(1) = 60 \pm 20$; at best, it passes two-photon terms at 60 times the rate it passes single-photon terms.

To show the coherent action of the filter, we set the input wave plate in mode a to rotate the linear polarization from horizontal to diagonal, creating the superposition of Eq. (1). We first measure the input state without the action of the Fock-state filter by blocking the ancilla photon in mode b, and performing tomography on mode c using detectors D3 and D4. Counting for 30 s per measurement setting, we measured raw twofold coincidence counts of {86, 68, 156, 61, 89, 77, 195, 61, 200, 170, 328, 131, 98, 102, 175, 71}. The reconstructed density matrix, shown in Fig. 3(c), gives us the initial state of the light and includes the effect of any birefringence in our experiment. The density matrix consists of near equal probabilities, and strong positive coherences between them—characteristic of the expected ideal state $|\psi\rangle = |\mathrm{DD}\rangle$. The fidelity between the ideal and measured state ρ is $\mathcal{F} = \langle\psi|\rho|\psi\rangle = (93 \pm 4)\%$; the linear entropy is $S_L = (11 \pm 8)\%$ [9], indicating the state is near-pure; and the tangle is zero within error, $T = (0.5 \pm 0.8)\%$, indicating that as expected the input state is unentangled.

The Fock-state filter is run by unblocking mode b and setting its coupler to the zero-delay position shown in Fig. 2. We performed tomography on the photon pairs at D3 and D4, but now in coincidence with the trigger and ancilla photon detectors, D1 and D2, counting for 8.25 hours per measurement setting, obtaining the raw counts {62, 10, 45, 25, 10, 59, 49, 49, 53, 40, 36, 45, 37, 50, 46,

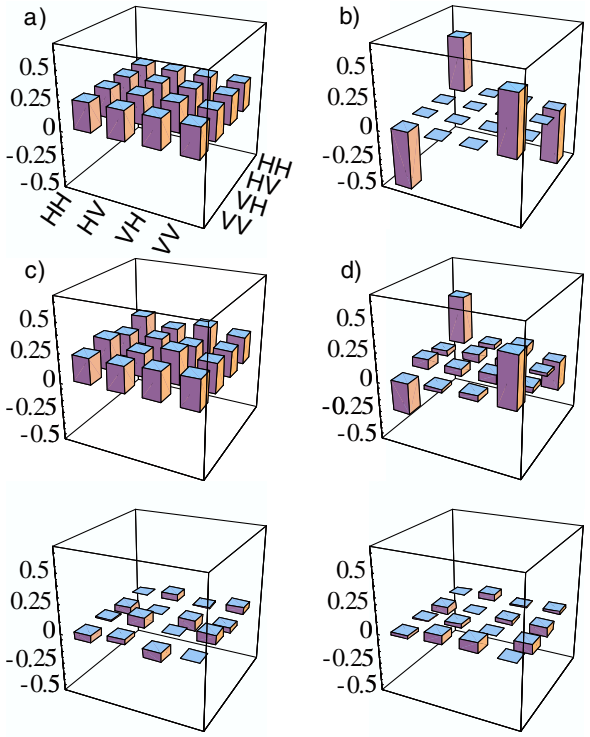

FIG. 3 (color online). Density matrices for the Fock-state filter. Ideal output states from the filter when the filtering is (a) turned off, $|DD\rangle$, and (b) turned on, $(|HH\rangle\text{-}|VV\rangle)/\sqrt{2}$, as described in text. The corresponding experimental tomographic reconstructions, based on raw counts, are shown, respectively, in (c) and (d), the upper (lower) panels are the real (imaginary) components. The fidelity between the ideal and measured states is $93 \pm 4\%$ and $69 \pm 9\%$, respectively. The state measured in (d) is entangled, with tangle $T = 20 \pm 9\%$.

72}. The reconstructed density matrix is shown in Fig. 3(d)]. Consistent with the prediction of Eq. (2) setting $\theta = \pi/4$, there are two striking differences between this and Fig. 3(c)]: (1) the dramatic reduction of the HV and VH populations and coherences; and (2) the sign change of the coherences between the HH and VV populations. The fidelity, between the ideal state, $|\psi\rangle = (|\mathrm{HH}\rangle - |\mathrm{VV}\rangle)/\sqrt{2}$, and the measured state ρ is $\mathcal{F} = (69 \pm 9)\%$. The linear entropy is $S_L = (57 \pm 6)\%$, the increase in entropy indicates that the filter introduces mixture but retains much of the input state's coherence. This is reflected in the output state entanglement, $T = (20 \pm 9)\%$, requiring coherence.

The tomography is based on the fourfold signal, which is particularly susceptible to background, due to low rates and long counting times. We use raw, rather than corrected fourfold counts, as unambiguous measurement of the background is nontrivial due to the manifold combinations of accidental detection events. Thus $(P_{\mathrm{HH}} + P_{\mathrm{VV}})/(P_{\mathrm{HV}} + P_{\mathrm{VH}})$ is a lower bound on the preferential absorption of the filter, 6.0 ± 1.5.

We have constructed a coherent nonlinear absorber—a Fock-state filter—combining measurement with higher-order quantum interference. The filter preferentially absorbed up to 60 times more single photons than photon pairs, and produced an entangled state from a separable state: the output was measured to have a tangle of $T = (20 \pm 9)\%$. By encoding quantum information in both number and polarization, we were able to succinctly demonstrate all the salient features of a Fock-state filter in a single experiment. This is a powerful technique suitable for applications requiring quantum nonlinear optics.

We thank Anton Zeilinger for valuable discussions. This work was supported in part by the DTO-funded U.S. Army Research Office Contract No. W911NF-05-0397, a UQ ECR Grant, and the ARC Discovery program.

Note added in proof.—While correcting the proofs, laboratory temperature stability and source brightness were both improved. Consequently, the Fock-state filter produced a more highly entangled state with tangle of $T = 51 \pm 11\%$, linear entropy of $S_L = 46 \pm 9\%$, and fidelity with the ideal of $\mathcal{F} = 77 \pm 6\%$. See additional online material [19] for details.

[1] E. Knill, R. Laflamme, and G. J. Milburn, Nature (London) **409**, 46 (2001).

[2] K. Sanaka, T. Jennewein, J.-W. Pan, K. Resch, and A. Zeilinger, Phys. Rev. Lett. **92**, 017902 (2004).

[3] T. B. Pittman *et al.*, Phys. Rev. A **64**, 062311 (2001); J. L. O'Brien *et al.*, Nature (London) **426**, 264 (2003); S. Gasparoni *et al.*, Phys. Rev. Lett. **93**, 020504 (2004).

[4] K. J. Resch *et al.*, Phys. Rev. Lett. **88**, 113601 (2002); A. I. Lvovsky and J. Mlynek, Phys. Rev. Lett. **88**, 250401 (2002).

[5] J. Wenger *et al.*, Phys. Rev. Lett. **92**, 153601 (2004); A. Zavatta *et al.*, Science **306**, 660 (2004).

[6] K. Sanaka *et al.*, Phys. Rev. Lett. **96**, 083601 (2006).

[7] H. F. Hofmann and S. Takeuchi, quant-ph/0204045; H. F. Hofmann and S. Takeuchi, Phys. Rev. Lett. **88**, 147901 (2002).

[8] B. M. Escher *et al.*, Phys. Rev. A **70**, 025801 (2004); K. J. Resch, Phys. Rev. A **70**, 051803 (2004); K. Sanaka, Phys. Rev. A **71**, 021801 (2005).

[9] D. F. V. James *et al.*, Phys. Rev. A **64**, 052312 (2001).

[10] Singles rate is the rate of single "clicks" from standard detectors and can arise from detection of one or more photons.

[11] C. K. Hong *et al.*, Phys. Rev. Lett. **59**, 2044 (1987).

[12] S. M. Tan *et al.*, Phys. Rev. Lett. **66**, 252 (1991); L. Hardy, Phys. Rev. Lett. **73**, 2279 (1994); D. T. Pegg *et al.*, Phys. Rev. Lett. **81**, 1604 (1998); J. Clausen *et al.*, Appl. Phys. B **72**, 43 (2001).

[13] C. Simon and J.-W. Pan, Phys. Rev. Lett. **89**, 257901 (2002); J.-W. Pan *et al.*, Nature (London) **423**, 417 (2003); P. Walther *et al.*, Phys. Rev. Lett. **94**, 040504 (2005).

[14] D. Bouwmeester *et al.*, Phys. Rev. Lett. **82**, 1345 (1999); A. Lamas-Linares *et al.*, Nature (London) **412**, 887 (2001).

[15] H. Lee *et al.*, *Quantum Imaging and Metrology: Proceedings of the Sixth International Conference on Quantum Communication, Measurement and Computing*, edited by J. H. Shapiro and O. Hirota (Rinton Press, Princeton, NJ, 2002), pp. 223–229.

[16] Alternatively, this can be seen as transforming a pair of identically polarized photons in the same spatial mode, $|2_D, 0_A\rangle$, to a pair of orthogonally polarized photons $|1_D, 1_A\rangle$, a nonlinear operation impossible with linear optical elements.

[17] $|\{D, A, R\}\rangle = (|0\rangle\{+, -, +i\}|1\rangle)/\sqrt{2}$.

[18] We used the same experiment to simultaneously measure both $n = 1$ and $n = 2$ absorption, unlike Ref. [6]. Our design ensured higher visibilities, $(95.20 \pm 0.02)\%$ and $(68 \pm 5)\%$, c.f. $83 \pm 1\%$ and $(61 \pm 6)\%$ [6], and significantly higher rates.

[19] See EPAPS Document No. E-PRLTAO-98-021711 for supplementary figures and text. For more information on EPAPS, see http://www.aip.org/pubservs/epaps.html.